Templating of Thin Films Induced by Dewetting on Patterned Surfaces

Kajari Kargupta and Ashutosh Sharma*

Department of Chemical Engineering, Indian Institute of Technology, Kanpur, UP 208 016, India

(Received 12 December 2000)

The instability, dynamics, and morphological transitions of patterns in thin liquid films on chemically heterogeneous striped surfaces are investigated based on 3D nonlinear simulations. The film breakup is suppressed on some potentially destabilizing nonwettable sites when their spacing is below a characteristic length scale of the instability, λ_h. The thin film pattern replicates the substrate surface energy pattern closely only when (i) the periodicity of substrate pattern lies between λ_h and $2\lambda_h$, and (ii) the stripe width is within a range bounded by a lower critical length, below which no heterogeneous rupture occurs, and an upper transition length above which complex morphological features unlike the substrate pattern are formed.

DOI: 10.1103/PhysRevLett.86.4536 PACS numbers: 47.20.Ma, 47.54.+r, 68.08.Bc, 68.15.+e

Self-organization during dewetting of thin films on deliberately tailored chemically heterogeneous substrates is of increasing promise for engineering of desired nanopatterns and micropatterns in thin films by templating [1–11]. On a chemically heterogeneous substrate, dewetting is driven by the spatial gradient of microscale wettability [12], rather than by the nonwettability of the substrate itself. The latter occurs in the so-called spinodal dewetting on homogeneous surfaces [13,14]. While the rupture of a thin film on a single heterogeneous patch is now well understood, patterned substrates pack a large density of surface features that are closely spaced. How does hydrodynamic interactions between the neighboring heterogeneities affect the pattern evolution dynamics and morphology in thin films? In this Letter, we address this question, which is central to our understanding of how faithfully the substrate patterns are reproduced in a thin film spontaneously: i.e., how effective is the templating of soft materials by the dewetting route and what are the conditions for ideal templating? An associated question for both the patterned and naturally occurring heterogeneous surfaces is whether all the potentially dewetting sites remain active or "live" in producing rupture when they are in close proximity. These questions are resolved based on 3D nonlinear simulations of the stability, dynamics, and morphology of thin films on periodic chemically heterogeneous surfaces.

The substrate considered consists of alternating less wettable and more wettable (or completely wettable) stripes that differ in their interactions with the overlying film. The key parameters of the substrate pattern are its periodicity interval (center-to-center distance between two consecutive stripes, L_p) and the length scale of the less wettable stripe (stripe width, W). The following nondimensional thin film equation governs the stability and spatiotemporal evolution of a thin film system subjected to the excess intermolecular interactions [12]:

$$\partial H/\partial T + \nabla \cdot [H^3 \nabla(\nabla^2 H)] - \nabla \cdot [H^3 \nabla \Phi] = 0. \quad (1)$$

$H(X, Y, T)$ is the nondimensional local film thickness scaled with the mean thickness h_o; $\Phi = [2\pi h_o^2/|A_s|] \times [\partial \Delta G/\partial H]$; ΔG is the excess intermolecular interaction energy per unit area, and A_s is the effective Hamaker constant for van der Waals interaction; X, Y are the nondimensional coordinates in the plane of the substrate, scaled with a length scale $(2\pi\gamma/|A_s|)^{1/2} h_o^2$; and the nondimensional time T is scaled with $12\pi^2 \mu \gamma h_o^5/A_s^2$; γ and μ refer to the film surface tension and viscosity, respectively. The terms (from left to right) in Eq. (1) correspond to the accumulation, curvature (surface tension), and the intermolecular forces, respectively. More details can be found elsewhere [12–14]. Briefly, the equation is valid for the Newtonian, nonslipping films, and therefore, in addition to the basic results obtained here, polymeric films could show additional rheological complexities. The length scale of the spinodal instability on a uniform surface is given by $\lambda = [-4\pi^2\gamma/(\partial^2 \Delta G/\partial h^2)]^{1/2}$. On a chemically heterogeneous striped surface, $\Phi = \Phi(H, X, Y)$. At a constant film thickness, we model the variation of Φ in the X direction by a periodic step function of periodicity, L_p. Gradient of force $\nabla\Phi$, at the boundary of the stripes, causes flow from the less wettable (higher pressure) stripes to the more wettable (lower pressure) stripes, even when the spinodal stability condition $\partial\Phi/\partial H > 0$ is satisfied everywhere [12]. It is known that a single stripe in the absence of its neighbors can cause rupture only if its width exceeds a critical length scale, $W_c \ll \lambda$ [12].

We consider general representation of antagonistic (attractive/repulsive) long-range and short-range intermolecular interactions applicable to the aqueous films [Eq. (2)] [14,15] and polymer films on high-energy surfaces such as silicon [Eq. (3)] [4,12,16]. In both cases, the long-range van der Waals force is stabilizing and thus films thinner (thicker) than a critical thickness are unstable (metastable):

$$\Delta G = -(A_s/12\pi h^2) + S_p \exp(-h/l_p). \quad (2)$$

For aqueous films A_s and S_p are both negative, denoting long-range van der Waals repulsion combined with shorter-range attraction, e.g., hydrophobic attraction [17]. On the hydrophobic stripes ($A_s^h = -1.41 \times 10^{-20}$ J,

 0031-9007/01/86(20)/4536(4)$15.00 © 2001 The American Physical Society

$S_p^h = -65$ mJ/m^2, and $l_p = 0.6$ nm), the film is spinodally unstable ($\partial\Phi/\partial H < 0$) below a critical thickness h_c of 7.4 nm. The equilibrium contact angle obtained from the extended Young-Dupre equation $\cos\theta = 1 + \Delta G(h_e)/\gamma$ is 61°, where h_e is the equilibrium thickness. On the hydrophilic stripes ($A_s = -1.41 \times 10^{-20}$ J, $S_p = -0.61$ mJ/m^2, and $l_p = 0.6$ nm), the film of any thickness is spinodally stable ($\partial\Phi/\partial H > 0$) and completely wets the surface.

Equation (1) was numerically solved using a central difference scheme in space combined with Gears algorithm for stiff equations for time marching and periodic boundary condition. The convergence of the results was verified by increasing the grid density and also by the use of nonuniformly spaced fine grids near the boundary of the stripes. The critical length W_c of a single heterogeneity (hydrophobic patch) that engenders rupture on a large hydrophilic substrate in this case is 0.08λ.

Ideal templating requires that dewetting should occur on every less-wettable site on the patterned substrate. Figure 1a shows a single rupture on a substrate containing four potentially dewetting sites ($n_S = 4$) when the periodicity interval is small, $L_p = 0.45\lambda$. The resulting lone drop spans across the remaining "inactive" hydrophobic sites. Figures 1a to 1c show an increased number of dewetted stripes ($n_D = 1, 2, 4$) and resulting liquid domains as L_p is increased from $0.45\lambda \rightarrow 0.68\lambda \rightarrow 0.9\lambda$. This, as well as a large number of simulations not displayed here, showed that, on a substrate containing many potentially destabilizing sites, only the sites (randomly picked) separated by a characteristic length scale of the instability, λ_h, of the order of the spinodal scale, λ, remain live or effective in causing the film rupture. Dewetting on the remaining intervening sites is suppressed since rupture on each site would require surface deformations on smaller scales resulting in a high surface energy penalty. The ratio of this characteristic length scale, λ_h, to the spinodal length scale, λ, obtained from simulations, decreases as the potential difference across the stripe boundary, ($\Delta\Phi$) increases (Fig. 2), where $\Delta\Phi = (\Phi^h - \Phi)$, evaluated at the initial thickness. A simple scale analysis ($H = 1 + \epsilon$, $\nabla^2\Phi \sim \Delta\Phi/cL^2$, $c < 1$), of Eq. (1) [12] leads to $\lambda_h/\lambda \propto [1 + \Delta\Phi/(-\epsilon c\,\partial\Phi/\partial H)]^{-0.5}$; and $\lambda_h \sim \lambda$ when the spinodal term $-\partial\Phi/\partial H$ is very strong compared to the applied potential difference. An interesting implication is that, even when the rupture occurs by the heterogeneous mechanism on a substrate containing a large density of heterogeneities, the length scale of the resulting pattern can give the illusion of spinodal dewetting by mimicking the characteristic length scale of the latter. Differentiating true spinodal dewetting from heterogeneous dewetting therefore requires a careful consideration of their distinct time scales and morphological features [12].

Since λ_h decreases with the decrease in the film thickness, a greater number of nonwettable heterogeneities become active in causing the film breakup for thinner films. Comparison of Figs. 1b (thickness = 6 nm, $\lambda = 0.67$ μm) and 1d (thickness = 5.5 nm, $\lambda = 0.42$ μm) clearly shows this for an identical substrate pattern. This transition uncovered based on dynamical simulations is also in conformity with the earlier equilibrium energy considerations [1] that are related, however, only to the equilibrium structures.

From the above discussion, a necessary condition for good templating is that $L_p \geq \lambda_h$ which ensures dewetting on every less wettable site ($n_D = n_S$). As shown below, this condition remains valid for other types of potential and also when both the stripes are nonwettable. However, in this case the contact line can move across the boundary of the stripes to the more wettable part. We simulated the 3D morphologies during the evolution of a polymerlike film on an oxide (low-energy) covered silicon (high-energy) substrate. An analytical representation of combined antagonistic (attractive/repulsive) long- and short-range intermolecular interactions for a polymerlike film on a coated (e.g., oxide covered) substrate is [12]

$$-12\pi\Delta G = [(A_s - A_{c1})/(h + d_{c1} + d_{c2})^2 + (A_{c1} - A_{c2})/(h + d_{c2})^2 + A_{c2}/h^2]. \quad (3)$$

A negative value of the effective Hamaker constant on the substrate ($A_s = A_s^h = -1.88 \times 10^{-20}$ J) signifies a long-range repulsion, whereas a positive value on coating ($A_{c1} = A_{c1}^h = 1.13 \times 10^{-20}$ J) represents an

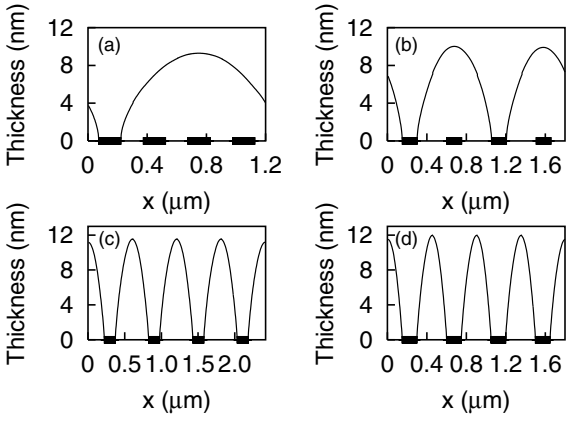

FIG. 1. Equilibrium thin film profile on a striped surface ($W = 0.16\lambda$). The less-wettable stripes are denoted by black rectangles. (a), (b), and (c) are for a 6 nm film for increasing periodicity. (d) shows the profile for a 5.5 nm thin film on a same substrate shown in (b).

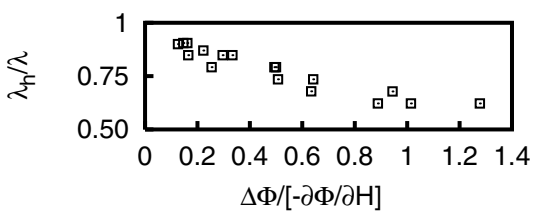

FIG. 2. Variation of the ratio of characteristic to spinodal length scale with the ratio $\Delta\Phi/(-\partial\Phi/\partial H)$, obtained from simulations using a different set of parameters.

intermediate-range attraction [12]. The nonwettable coating (e.g., oxide) thickness ($d_{c1} = 2.5$ nm, $d_{c1}^{h} = 4$ nm) is increased on alternating stripes which causes the macroscopic contact angle to increase from 0.58° on the more wettable stripes to 1.7° on the less wettable stripes. A still shorter-range repulsion may arise due to a chemically adsorbed or grafted layer of the polymer ($A_{c2} = -0.188 \times 10^{-20}$ J, $d_{c2} = 1$ nm are the film Hamaker constant and the thickness of the adsorbed layer, respectively) [12]. The representation, Eq. (3), is chosen for illustration without affecting the underlying physics, which we have verified for many different potentials.

Figures 3A–3D depict the effect of the periodicity interval, L_p, on the self-organization of a 5 nm thin film that is spinodally unstable on both types of stripes. In each case, the evolution starts with local depressions on the less-wettable stripes (Figs. 3A–3D). For L_p sufficiently smaller than λ ($L_p = 1$ μm, $\lambda = 1.51$ μm based on $\gamma = 38$ mJ/m^2 and $\mu = 1$ kg/m s), the isolated holes or depressions that form along the less-wettable stripes grow onto the more-wettable regions and coalesce with each other rapidly (Fig. 3A) leading to a disordered structure and very poor templating. Increasing periodicity ($L_p = 1.2$ μm; Fig. 3B) leads to more ordered dewetting, but the number of dewetted regions remain less than the number of less-wettable stripes, and defects evolve at late times (e.g., holes in the liquid ridge; image 4 of Fig. 3B). For $L_p \geq \lambda$ (Figs. 3C and 3D), the number of dewetted stripes equals the number of less-wettable stripes. However, templating in the form of liquid ridges with straight edges is best at an intermediate periodicity, $L_p \sim \lambda_h$ (Fig. 3C). A further increase in L_p makes the width of the dewetted region bigger than the width of the less-wettable stripe (image 4 of Fig. 3D), i.e., the contact line resides in the interior of the more wettable stripe, rather than close to the boundary.

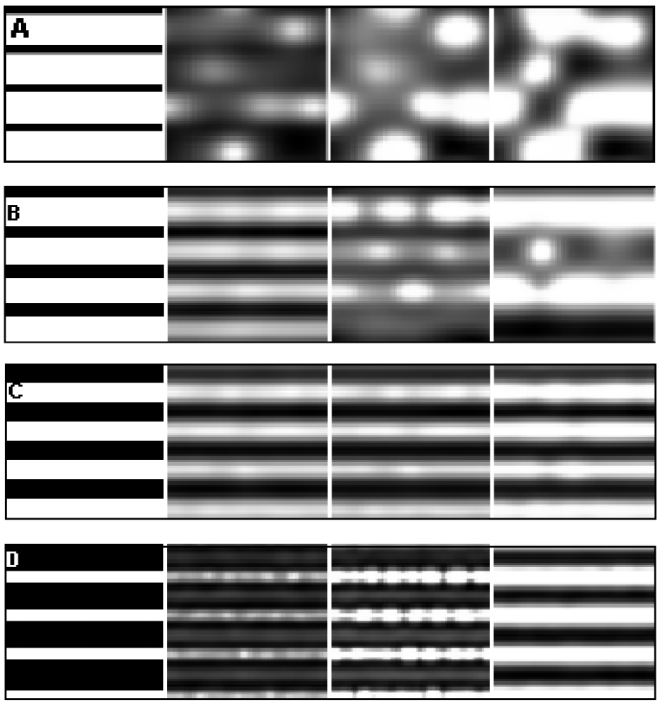

FIG. 3. Morphological evolution in a 5 nm thick film on a striped surface ($W = 0.8$ μm $= 0.53\lambda$). In (A)–(D), periodicity of surface pattern L_p are 1, 1.2, 1.45, and 3 μm, respectively. The first image in this figure, as well as in the subsequent figures, represents the substrate surface energy pattern; black and white represent the more wettable part and the less wettable part, respectively. For other images describing the film morphology, a continuous linear gray scale between the minimum and the maximum thickness in each picture has been used.

The transition of surface morphology can also be clearly understood from Fig. 4, which shows that ideal templating occurs for an intermediate thickness (Fig. 4B) for which the spinodal wavelength, $\lambda(= 3$ μm) is equal to L_p. Thinner films evolve by the formation of droplets on the more wettable stripes due to the spinodal mechanism assisted by the Rayleigh instability. For thicker films ($\lambda > L_p$), dewetting occurs on fewer stripes with the formation of holes in broad liquid ridges (e.g., Fig. 4C).

We found that, besides L_p, the other parameter that governs the thin film pattern is the stripe width (W). Figures 5A–5D show the transition of patterning with the increase of the stripe width (W), keeping the periodicity, L_p, fixed ($>\lambda$). For small stripe width ($\sim 0.4\lambda$; Fig. 5A), rupture is initiated at the center of less wettable stripes by the formation of depressions that coalesce to form rectangular dewetted regions of widths greater than the stripe width. For a larger stripe width ($W \sim 0.8\lambda$), dewetting is initiated by a layer of holes at each of the two boundaries of the stripe (image 2 of Fig. 5B). Coalescence of these two layers of holes leads to the dewetted regions containing some residual droplets (image 4 of Fig. 5B). Further increase in the stripe width leads to the formation of two layers of holes on each stripe separated by an elevated liquid cylinder (image 2 of Fig. 5C). Thus, at an intermediate stage of evolution, the number of cylindrical liquid ridges becomes twice the number of more wettable stripes on the substrate (image 3 of Fig. 5C). Eventually, liquid ridges on the less-wettable region disintegrate into droplets (not shown). Laplace pressure gradients cause ripening of the structure leading to the merging of droplets with the liquid ridges (image 4 of Fig. 5C). Further increase in the stripe width breaks the whole order of the substrate pattern due to the formation and repeated coalescence of several layers of holes on each stripe that eventually evolve into arrays of irregular droplets. Thus, a good synchronization of the thin film morphology with the substrate pattern requires

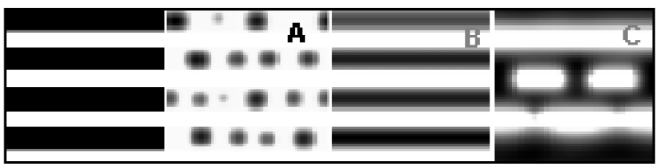

FIG. 4. 3D morphologies at late stages of evolution for films of thickness (A) 2.5 nm, (B) 6.9 nm, and (C) 8 nm on a striped surface with $W = 1.2$ μm and $L_p = 3$ μm.

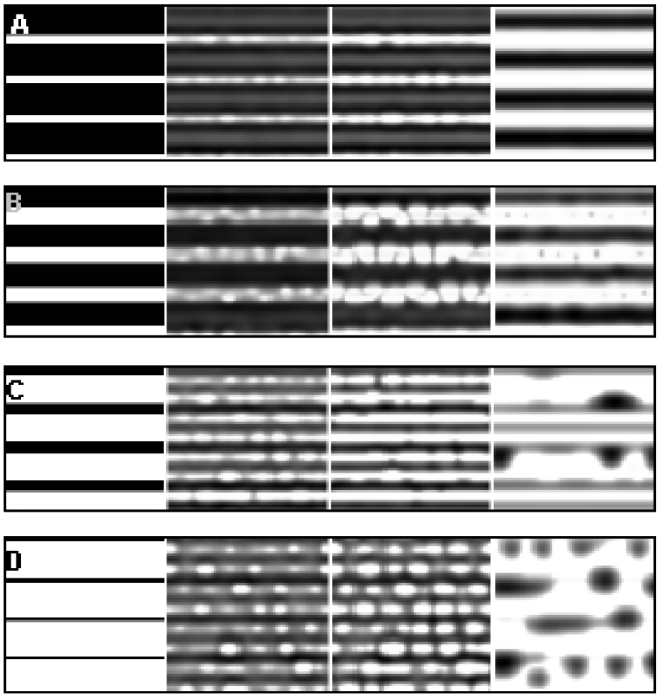

FIG. 5. Morphological evolution in a 5 nm thick film on a striped surface ($L_p = 3\ \mu\text{m} \sim 2\lambda$). $W = 0.6$, 1.2, 2.1, and 2.7 μm, respectively, for (A)–(D).

an upper limit on the stripe width, W_t, and a breakdown of templating due to the off-center dewetting occurs for $W > W_t$ (boundary 3 in Fig. 6).

In conclusion, the 3D thin film morphology on a patterned substrate during dewetting can be modulated profoundly by a competition among the time scales (spinodal and heterogeneous) and length scales (spinodal, stripe width, periodicity, thickness) of the problem. On a striped substrate, ideal templating in the form of cylindrical liquid ridges covering the more wettable stripes occurs when (shaded region in Fig. 6) (i) periodicity, L_p, lies between λ_h and $2\lambda_h$ (boundaries 2 and 4 in Fig. 6), (ii) the stripe width is larger than a critical width, W_c, which is effective in causing rupture by the heterogeneous mechanism, but smaller than a transition width, W_t, that ensures initiation of dewetting at the stripe center (boundaries 1 and 3 in Fig. 6), and (iii) the contact line remains close to the stripe boundary. Even a very weak wettability contrast (e.g., Fig. 3) is sufficient to align the thin film pattern with the template under the above conditions. Predictions of our simulations show close resemblance to the recently reported experimental observations on dewetting of polymers on patterned surfaces that reveal (i) best templating for an intermediate thickness film [6,10] and (ii) correspondence between the natural length scale and periodicity of the substrate pattern for good templating [4–6]. Finally, on a substrate containing many potentially destabilizing sites, only the sites separated by a characteristic length scale, $\lambda_h(\sim\lambda)$, remain live or effective in causing the film rupture. It is hoped that this study will help in the design and interpretation, creation, and

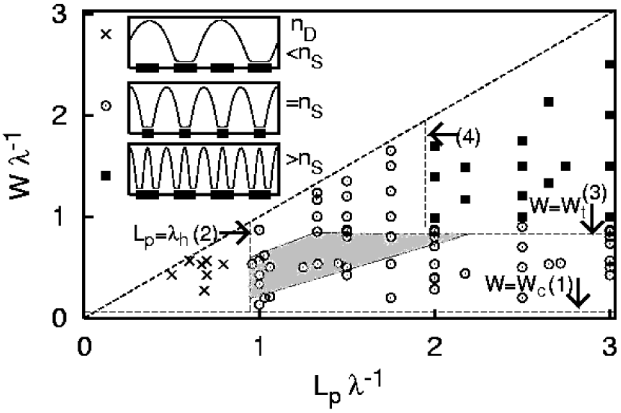

FIG. 6. Morphology diagram for the potential of Eq. (3). The broken lines, 1, 2, 3, and 4, denote the boundaries between different regimes at the onset of dewetting as shown in the figure by three symbols. The shaded region corresponds to good templating such that $n_D = n_S$, $W_c < W < W_t$, and the contact line is located at the stripe boundaries. Insets show patterns corresponding to the three symbols shown.

rational manipulation of self-organized microstructures in thin films by templating.

Discussions with G. Reiter are gratefully acknowledged.

*Email address: ashutos@iitk.ac.in

[1] P. Lenz and R. Lipowsky, Phys. Rev. Lett. **80**, 1920 (1998); P. Lenz and R. Lipowsky, Eur. Phys. J. E **1**, 249 (2000); R. Lipowsky, P. Lenz, and P. S. Swain, Colloids Surf. A **161**, 3 (2000).
[2] H. Gau *et al.,* Science **283**, 46 (1999).
[3] A. Kumar and G. M. Whitesides, Science **263**, 60 (1994).
[4] L. Rockford *et al.,* Phys. Rev. Lett. **82**, 2602 (1999).
[5] M. Boltau *et al.,* Nature (London) **391**, 877 (1998).
[6] M. Nisato *et al.,* Macromolecules **32**, 2356 (1999).
[7] M. Gleiche, L. F. Chi, and H. Fuchs, Nature (London) **403**, 173 (2000).
[8] D. E. Kataoka and S. M. Troian, Nature (London) **402**, 794 (1999).
[9] A. M. Hlggins and R. A. L. Jones, Nature (London) **404**, 476 (2000).
[10] A. Karim *et al.,* Phys. Rev. E **57**, R6273 (1998).
[11] G. Lopez *et al.,* Science **260**, 647 (1993).
[12] R. Konnur, K. Kargupta, and A. Sharma, Phys. Rev. Lett. **84**, 931 (2000); K. Kargupta, R. Konnur, and A. Sharma, Langmuir **16**, 10243 (2000).
[13] G. Reiter, R. Khanna, and A. Sharma, Phys. Rev. Lett. **85**, 1432 (2000); S. Herminghaus *et al.,* Science **282**, 916 (1998); A. Oron, Phys. Rev. Lett. **85**, 2108 (2000).
[14] A. Sharma and R. Khanna, Phys. Rev. Lett. **81**, 3463 (1998).
[15] U. Thiele, M. Mertig, and W. Pompe, Phys. Rev. Lett. **80**, 2869 (1998); A. S. Padmakar, K. Kargupta, and A. Sharma, J. Chem. Phys. **110**, 1735 (1999).
[16] H. I. Kim *et al.,* Phys. Rev. Lett. **82**, 3496 (1999).
[17] C. J. Van Oss, M. K. Chaudhury, and R. J. Good, Chem. Rev. **88**, 927 (1988).